coatings

MDPI

Article

Dependence of Electrical Charge Transport on the Voltage Applied across Metal–Graphene–Metal Stack under Fixed Compressing Force

Tomas Daugalas *, Virginijus Bukauskas, Algimantas Lukša, Viktorija Nargelienė and Arūnas Šetkus

Department of Physical Technologies, Center for Physical Sciences and Technology (FTMC), Saulėtekio Ave. 3, LT-10257 Vilnius, Lithuania

* Correspondence: tomas.daugalas@ftmc.lt

Abstract: While charge transport in the horizontal plane of graphene has been widely studied, there is only limited understanding about the transport across a stack of films that include graphene sheets. In this report, a model of a metal–graphene–metal stack was produced and investigated via detailed analysis of experimental dependences of electrical current on applied external voltage. Scanning probe microscopy (SPM) was used to measure the dependences of the local tunneling current on the voltage under fixed compressing force. The SPM platinum probe produced the compressing force on gold-supported graphene in the metal–graphene–metal system. The experimental results were explained by a model that included the pinning of the Fermi level of graphene to platinum and the related changes in the parameters of the potential barrier for the electron flow. It was demonstrated that low-voltage and high-voltage intervals can be identified in the charge transport across the metal–graphene–metal stack. In the high-voltage interval (approximately > $|\pm 0.7|$ V in the tested stack), the history of the current measurement was detected due to the charge accumulation. In the low-voltage interval, the current was determined by the electronic states near the Fermi level. In this interval, the graphene layer can function as a blocking gate for the electron transport in the metal–graphene–metal system.

Keywords: monolayer graphene; Van der Waals junction; electron transport; nanoscale modification; Fermi level pinning

check for updates

Citation: Daugalas, T.; Bukauskas, V.; Lukša, A.; Nargelienė, V.; Šetkus, A. Dependence of Electrical Charge Transport on the Voltage Applied across Metal–Graphene–Metal Stack under Fixed Compressing Force. *Coatings* **2023**, *13*, 1522. https://doi.org/10.3390/coatings13091522

Academic Editor: Dimitrios Tasis

Received: 8 August 2023
Revised: 25 August 2023
Accepted: 28 August 2023
Published: 30 August 2023

1. Introduction

Integration of two-dimensional (2D) materials in three-dimensional (3D) electronic devices with metal contacts is one of the main challenges in the development of highly integrated combined systems. These systems can be highly attractive due to tunable electronic properties, enhanced device performance, novel physical phenomena, integration with existing technologies, and versatile applications [1,2]. Special attention is brought to the use of 2D dielectric films, which show high potential as a key part in flexible electronic device development [3] alongside new designs of electronic and optoelectronic devices, such as transistors, barristors, photodetectors, photovoltaics, and light-emitting devices with unique characteristics and functionalities [4]. A number of works have proved that 2D–3D metal–graphene interface properties are of high interest for various applications, ranging from systems fabricated by epitaxial growth to bulk metal–graphene-based structures [5]. However, the lack of knowledge in the physics of 2D–3D material interfacial properties under applied external voltage is a key objective to overcome for successful targeted device creation. Therefore, the influence of electric fields on the interactions in metal–graphene interfaces was investigated over the last decade [6,7]. It was shown that the contact resistivity of a metal–graphene system strongly depends on the bias voltage across the metal–graphene junction [8,9]. For metal–graphene-type systems, contacting interfaces with physical isolation and weak interactions can act as potential barriers for electrical conduction [10]. Depending on the barrier parameters, the change of the tunneling mechanism can occur if sufficient voltage is applied across the junction [11,12]. If the height of the barrier is high enough that the change in its shape upon the applied external electric field does not influence the tunneling mechanism, charge redistribution of the charge carriers can occur along the layers, induced by a potential gradient normal to the interface [13]. Such charge redistribution can significantly impact the band edge positions and, therefore, the charge transport properties. According to the first principles DFT calculations in the metal–graphene–metal (M-G-M) system, it was found that the electron density distribution tends to stay on both the metal and graphene sides rather than being concentrated at the interface region. Thus, an interface dipole is developed, as a consequence of intramaterial charge redistribution, regardless of whether intermaterial charge transfer takes place or not [14].

Theoretical works have provided insight into charge redistribution in metal–graphene complexes occurring at different rates for various contact materials [15], thus determining the differences in conductivity across M-G-M interfaces with different components [16].

As the main focus for studies is on single-metal–graphene interface charge transfer, there is still a lack of knowledge on charge transfer in double-interface metal–graphene–metal systems. Therefore, in this work, charge transfer in a metal–graphene–metal system was investigated using the scanning probe microscopy technique under mechanical pressure and applied external voltage. The charge transport was investigated by applying various external voltages during force spectroscopy and I-V measurements in the M-G-M stack. The results proved an asymmetrical built-in charge distribution in the system, which was explained by a model with Fermi level pinning effect in the system.

2. Materials and Methods

Metal–graphene–metal stacked structure was investigated under the applied force with a constant electric field set between metal electrodes. The stack was constructed on a standard Si plate with an insulating SiO_2 layer (thickness d_{SiO2} = 275 nm) (SIEGERT WAFER Gmbh, Aachen, Germany). A thin Au layer was formed on the Si plate using DC magnetron sputtering. Commercial chemical vapor deposition (CVD)-grown graphene monolayer (Graphenea) was then transferred via standardized wet transfer method on the Au film [17]. Pt probe (Pt-rock, model RMN12Pt400B, Bruker, Billerica, MA, USA) was placed on top of the structure and used as an electrode for measurements. The second electrode was the Au film with thickness up to 100 nm, where the voltage was applied, and the polarity changed with respect to the Pt probe electrode. The schematics of sample composition are shown in Figure 1.

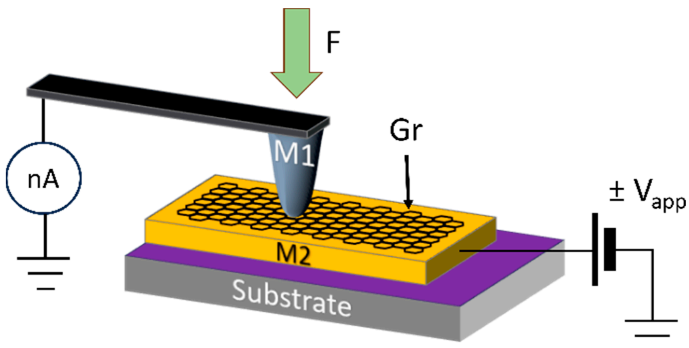

Figure 1. Metal–graphene–metal structure with applied voltage and compressing force.

In this study, we focused on electrical measurements conducted in specific areas of the sample where a monolayer graphene sheet covered the gold surface. Figure 2b illustrates the typical surface morphology at the edge of the monolayer graphene, acquired by atomic force microscopy (AFM) (Veeco Inc., Edina, MN, USA). The dashed blue line demarcates the boundary between the bare Au surface on the left and the graphene-covered Au on the right. To provide a more definitive indication of the presence of graphene, the phase lag of the cantilever vibration was examined, as demonstrated in Figure 2a. The phase lag is influenced by surface properties such as adhesion, friction, and viscoelasticity [18]. As shown in Figure 2a, there is a notable difference in the phase lag between the bare Au surface and the graphene-supported Au film, amounting to approximately 10 degrees. Previous RAMAN spectroscopy studies confirmed that the areas represented by darker regions in the scanned phase image (Figure 2a) indicate the presence of the graphene layer [17]. The cross-section (Figure 2c) along the red solid line in Figure 2b reveals that the distance between the nearest peaks or valleys exceeds the radius of the SPM tip used in our experiments, typically falling within the range of 5–55 nm. More details on the reconstruction of the SPM tip shape can be found in [19]. Considering both the surface morphology and the shape of the SPM probe tip used in our experiments, the influence of sample surface roughness on the electrical measurements can be neglected. Additionally, a detailed analysis of the Pt probe influence to the measurements for the same experiment series was provided previously by Daugalas et al. [20].

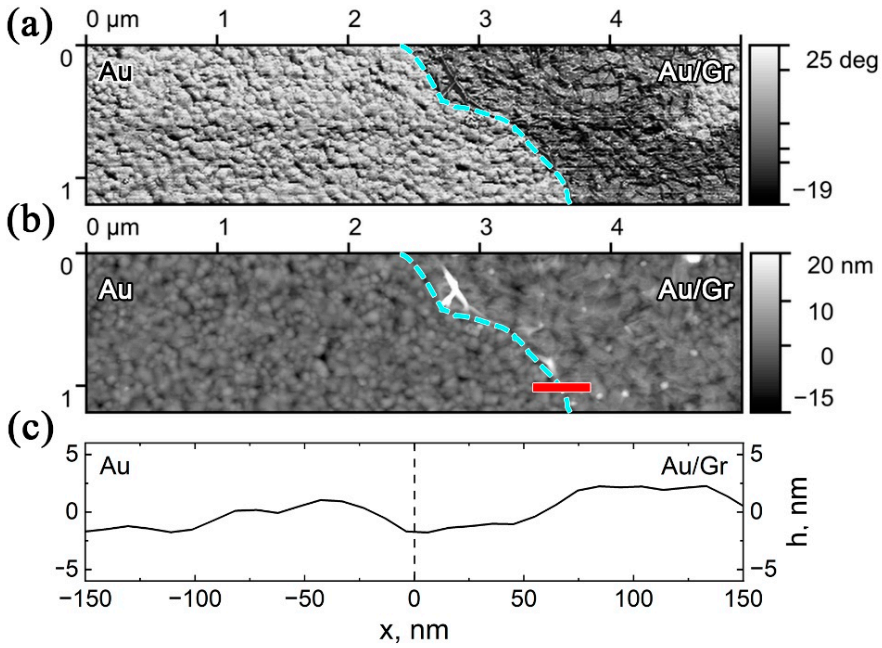

Figure 2. AFM Phase lag (**a**) and topography (**b**) maps with division (dashed blue line) of graphene covered Au film (right side) and bare Au film (left side). Depicted below is the cross-section of graphene covered and bare Au film at the boundary between the areas (red solid line) (**c**).

Experiments on samples were performed using a Dimension 3100 Scanning Probe Microscope (SPM) (Veeco Inc., Edina, MN, USA) with an additional TUNA (Veeco Inc.) module for electrical measurements. A reference PG (Platinum Grating, Bruker, Billerica, MA, USA) plate was used for electrical calibration of the probe before and throughout the experiments.

Local tunneling current was measured in the stack-like metal–graphene–metal structure with applied external voltage. Depending on the group of the experiments, the voltage was varied according to individual programs within the interval -1.5 V $\leq V_{app} \leq +1.5$ V. Three modes of the programs were used.

One mode of the current–voltage measurements included permanent scanning of both the current and the compressing force at once under fixed external voltage. The compressing force was varied within the interval $0 < F < 100$ nN. This approach was identified using the F-ramp mode. Additionally, this mode was used to scan current and force simultaneously during probe retraction movement.

A modification of the F-ramp mode (F*-ramp) was used for measuring the adhesion force F_{adh} between the sample and the probe with an applied fixed external voltage. The force was measured at the jump-off triangle apex in the SPM force curve during probe retraction movement.

In the third group of the experiments (F-stable mode), a constant voltage was applied to the system during the complete cycle that included landing and retracting of the metal probe on/from the gold supported graphene surface. The electrical current was measured for a stable probe–surface contact produced by a delicate pressing probe to the surface. The compression force was set at the same magnitude by fixing the set-point of the probe in the scanning probe microscope. The force was reliably reproduced to fix the contact at about F_0 = (30 ± 20) nN in this type of experiments. For such contact, the current–voltage data point was measured at the constant voltage. A set of the points was obtained by changing the voltage magnitude in each sequential probe landing.

The voltamperic characteristics were obtained when the current versus voltage was measured by ramping voltage from the minimal to the maximum under fixed compressing force. The probe was pressed to the surface by constant force from the interval $0 < F < 400$ nN, which was proven to cause minimal to no effect on the system and measurement results by Daugalas et al. [19], in this I-V measurement mode.

The force values for all the measurements were changed with a step of ΔF_{step} = (2 − 3) nN.

3. Results and Discussion

3.1. Electrical Current Characteristics of M-G-M System

Electron transport through the graphene sheet between two metal electrodes in the M-G-M structure was investigated experimentally during the SPM probe landing on the sample surface. Typical dependences of electrical current I_T on the compression force F were illustrated in Figure 3a,b. The dependences were measured for constant applied voltages 0.4 V and −0.4 V, which were low enough not to cause long term effects on the system yet high enough to provide sufficient data, as previously shown by Daugalas et al. [20].

Figure 3a displays the results of measurements conducted within a comparably low voltage $V_L < 0.5$ V. An asymmetry in the changes of the current signal I_T ($I_T > 0.1$ nA) was observed for different voltage polarities. Given that the applied external voltage was too low to significantly shift the Fermi level E_F, one would expect the I_T dependence on compression force to be symmetrical for positive and negative voltages. However, the observed asymmetry can be explained by the presence of built-in charge distribution across the M-G-M structure, resulting from differences in the metal contacts [8].

Experiments with applied voltages of up to $|V_H| < \pm 1.5$ V also displayed asymmetry in the changes of the current signal I_T. The results for several voltage values were depicted with a constant ΔI_T = 1500 nA shift in Figure 3b for clarity. The difference in metal contacts and the built-in charge distribution here explains the stable asymmetry in current signal, as only the applied voltage was changed. The current signal above noise level ($I_T > 0.1$ nA) shift towards lower compression force with the increase in the applied voltage V_H was previously explained for the M-G-M system by Daugalas et al. [19].

The typical direct measurement of I-V characteristics at constant compression forces, using I-V measurement mode in low voltage range, was performed to distinguish the voltage and mechanical compression influence on the charge transport. The compression force values were selected to display the non-monotonous dependence of current in the system with regard to compressing force of the system at similar and different forces, as was previously shown by Daugalas et al. [19]. The I-V curves displayed linear dependencies with regard to applied low voltage in the range of $|V_{VL}| < \pm 40$ mV as displayed in Figure 3c. Since the applied voltages were insufficient to shift the E_F in the system, the change in conductivity is attributed only to the acting compression force F that changes the distance between the graphene and metals.

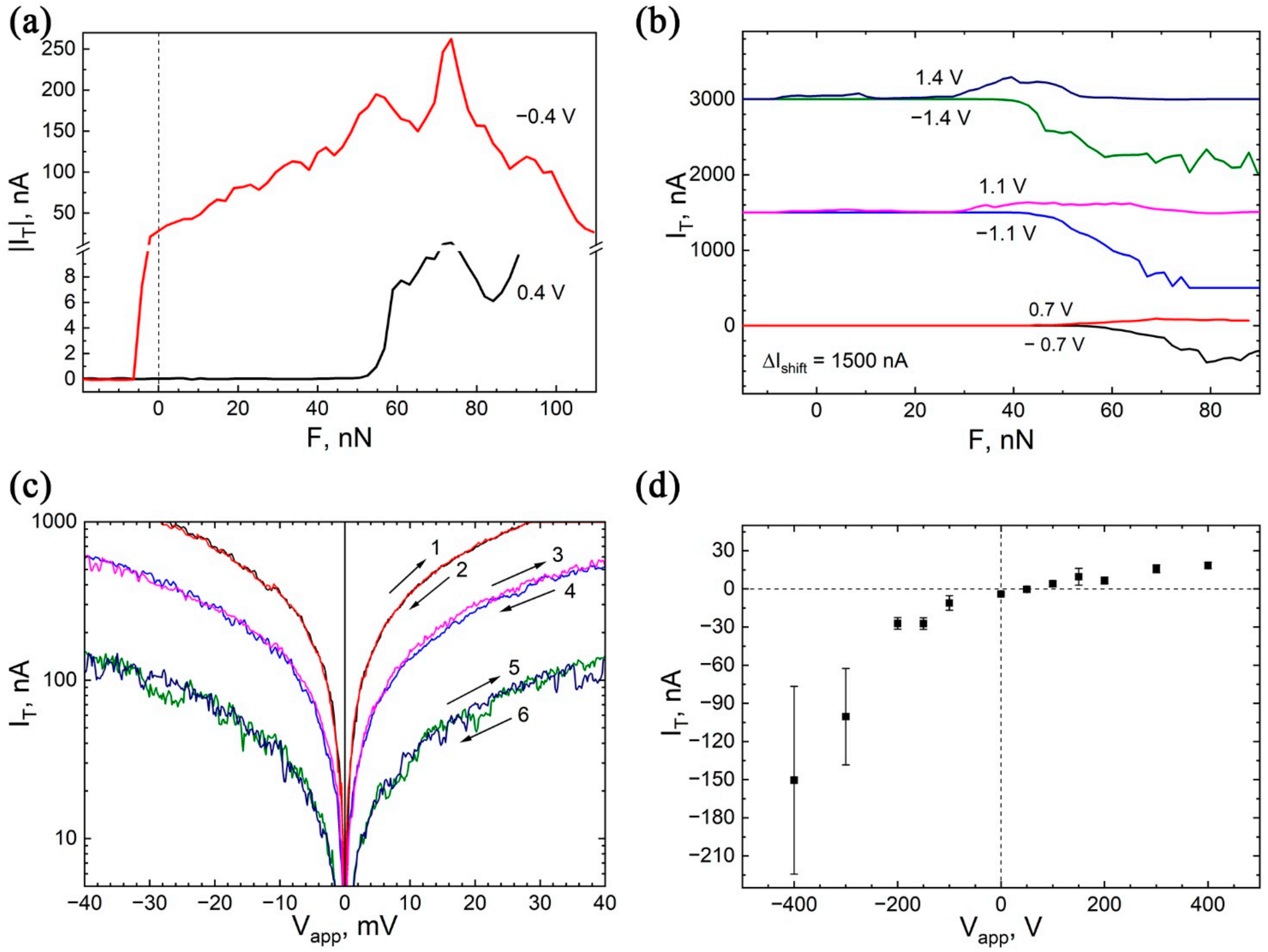

Figure 3. Electrical current dependence of Au-G-Pt system on applied force for V_L (**a**) and various V_H (**b**) applied voltages. (**c**) Electrical current dependence on applied external voltage using I-V measurement mode for compression forces $F_{1,2}$ = 373 nN, $F_{3,4}$ = 390 nN, and $F_{5,6}$ = 71 nN. The arrows show voltage sweep direction for trace (upwards) and retrace (downwards) directions. (**d**) Electrical current dependence on applied external voltage from F-stable measurement mode at F_0 = (30 ± 20) nN.

The influence of applied voltage to charge transfer in the M-G-M system was investigated by measuring I-V characteristics in the F-stable mode. A fixed single compression force F_0 = (30 ± 20) nN was applied to the tested system under the applied voltages $|V_{app}| \leq \pm 0.4$ V. The current dependence on the applied voltage showed a diode-like I-V characteristic, which was depicted in Figure 3d. The current I_T showed non-linear behavior, with higher values when the negative potential was applied to the Au film. The presence of asymmetric I-V characteristics in the M-G-M system can be explained by several factors, and one of the reasons is the difference in work function of the metals attached to the graphene layer. This work function difference can lead to variations in the electronic properties and charge transfer at the metal–graphene interfaces. Furthermore, the redistribution of charges between the metal and graphene layers significantly impacts the electrical conductivity of the system [21]. The interaction between the applied external voltage and the charge redistribution alters the carrier concentration in the graphene layer. As a result, the electrical conductivity of the M-G-M system experiences modifications, contributing to the observed asymmetric I-V characteristics.

To investigate whether the applied external electric field alters the charge distribution within the M-G-M system, measurements of the charge-dependent parameters were performed. Based on the model described in [20] such parameter can be detach force between the graphene surface and SPM probe.

3.2. Detach Force as an Indication of Charge Distribution Changes

The dependencies of the charge-sensitive detachment force on the applied voltage were examined through individual force curve cycles. By applying an external electric field of a fixed magnitude to the metal–graphene–metal system, excess charges can be introduced. These charges have a direct impact on the forces involved in the interaction between the probe and the sample [20]. The relation between applied external voltage and the probe-sample interaction forces was measured using a modified F*-ramp measurement mode. Typical results of detach force dependency on the applied external voltage with corresponding voltage change sequences are illustrated in Figure 3. Two different applied voltage change sequences are shown in Figure 4c,d.

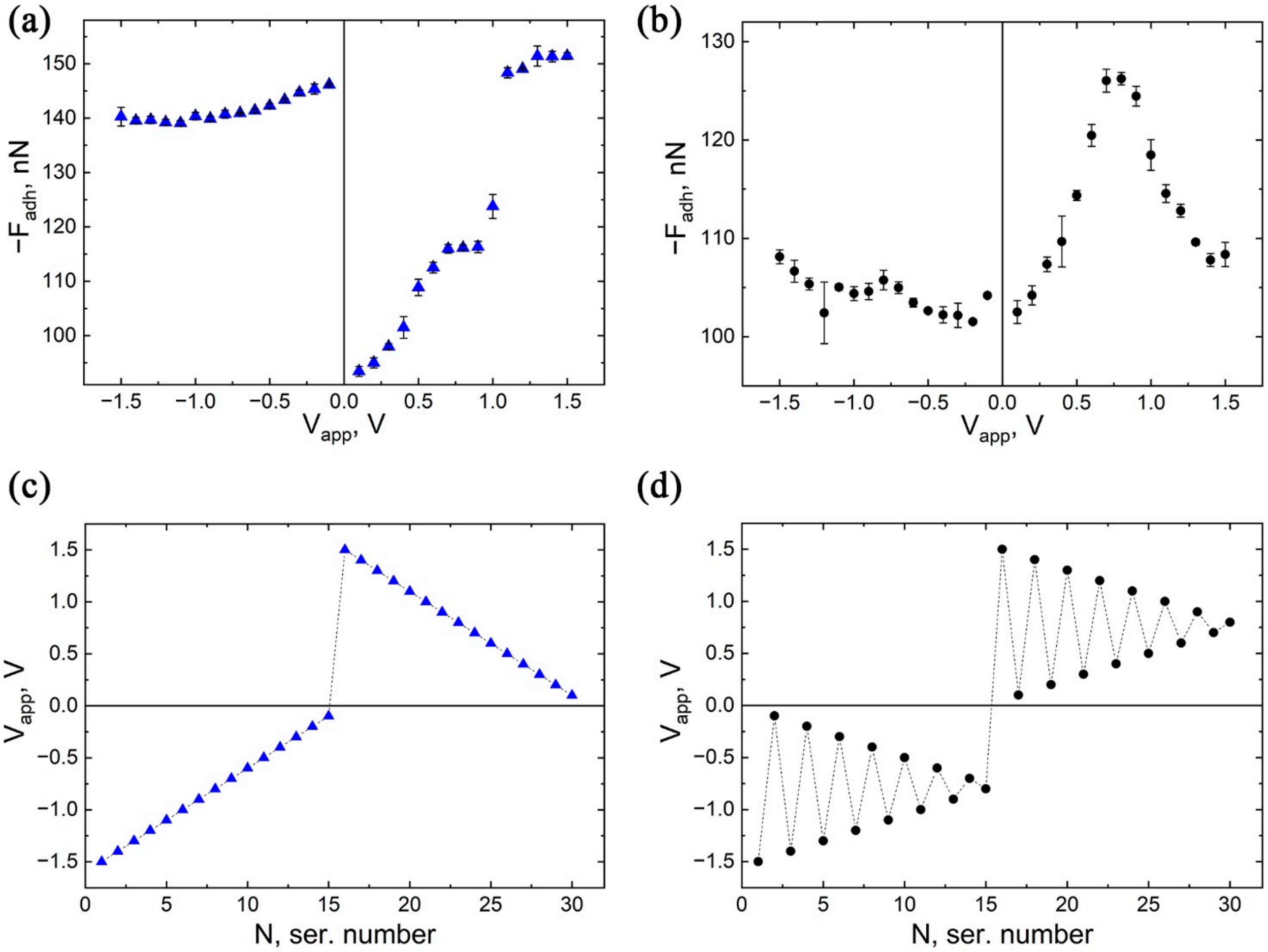

Figure 4. Dependence of the tip–surface interaction force at the jump-off triangle apex in the SPM force curve experiments on external applied DC voltage (**a**,**b**). Corresponding to the (**a**,**b**) step-like change in magnitude of V_{app} with increasing serial number of the force curve cycle in the consecutive measurement of the tip-surface interaction force are shown in (**c**,**d**), respectively.

The presence of asymmetrical charge distribution within the M-G-M system results in the accumulation of charges at the specific distances of interfaces between graphene and metal [14]. This behavior can be elucidated by observing changes of detach force F_{adh} for a special applied voltage V_{app} algorithms. With the negative voltage applied and the system set in the forward bias state, the probe-sample interaction force showed weak correlation with the applied voltage value, as seen from Figure 4a,b. The F_{adh} was found to be stable at $|F_{adh}|$ = (145 ± 5) nN and $|F_{adh}|$ = (105 ± 5) nN for linear (Figure 4c) and zig-zag (Figure 4d) voltage sequences respectively. The relatively constant F_{adh} value at negative applied voltage indicated no significant additional electrostatic charge acting on the Pt probe.

The application of positive voltage to the system displayed the probe-sample interaction change with regard to the applied voltage sequence. The observed sudden drop in detach force at an applied voltage V_{app} of approximately 1 V (as shown in Figure 4a) occurs when the positive voltage is decreased according to the algorithm depicted in Figure 4c. This drop can be attributed to changes in the M-G-M system due to charge redistribution induced by relatively high external voltages. Previous research by Daugalas et al. [20] has demonstrated that voltages lower than 0.5–0.7 V do not significantly alter the M-G-M system. Therefore, it can be inferred that measurements conducted at lower voltages serve as a scanning signal. Furthermore, when V_{app} > 1 V is applied, it induces significant changes in the M-G-M system, which can be detected through the measurement of detach force. Importantly, the true state of the system, after being influenced by higher voltages, can only be accurately identified by reducing the measurement voltage. This implies that when the measurement voltage is sufficiently high to induce changes in the system, reducing the voltage provides a means to probe and discern the actual state of the system.

Indeed, an alternative measurement algorithm displayed in Figure 4d provides further visualization of the effect. In this case, the external voltage applied to the M-G-M system undergoes successive changes from a "forming" state to a "scanning" state. The dependence of the detach force on V_{app} differs from that shown in Figure 3a, highlighting distinct behavior. As depicted in Figure 4b, the detach force initially increases as V_{app} increases, similar to the observations in Figure 4a, up to a range of 0.7–0.8 V. However, for V_{app} values greater than 1 V, the detach force exhibits a decrease as V_{app} increases. This can be explained by changes in the charge distribution within the M-G-M system upon the application of high voltages. Notably, unlike the behavior observed in Figure 4a, the system partially reverts to the initial state after the low voltage is applied.

3.3. Electrical Current Changes Retracting the SPM Probe from the Surface

The applied external voltage-induced changes in electric charge within the M-G-M interfaces can have a significant impact on the electrical contact between the layers [8]. These changes can be detected by measuring the electrical current I_T in F-ramp mode while the SPM probe retracts. Figure 5 illustrates the dependencies of I_T on the probe-sample force under different applied voltages.

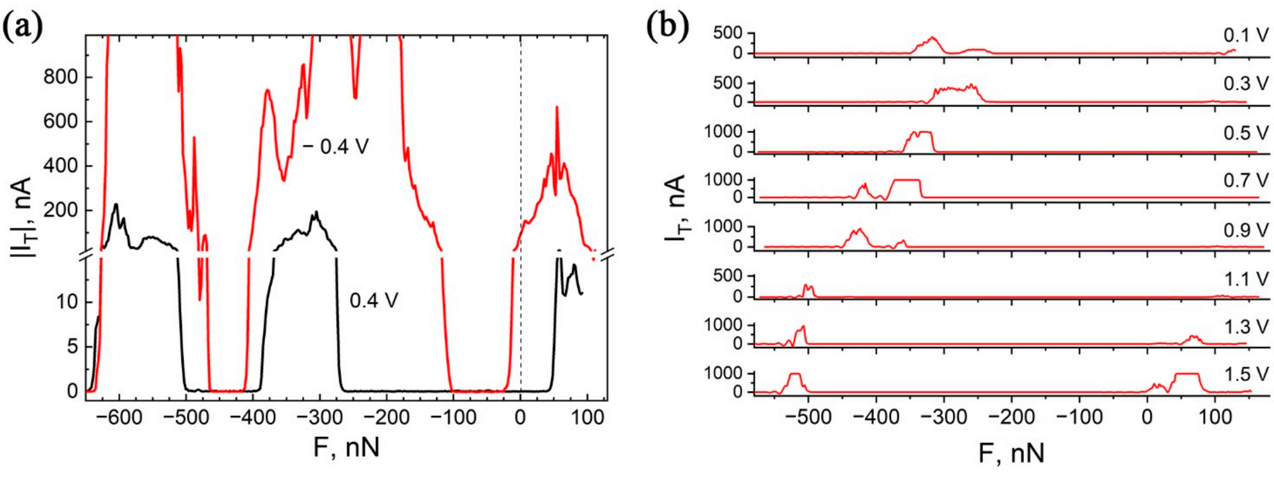

Figure 5. Electrical current dependence of Au-G-Pt system on probe acting force during retract movement from the sample surface for specific V_{app} = ±0.4 V (**a**) and extended positive voltage range of up to V_{app} < 1.5 V (**b**).

The asymmetry in electron transfer between the Pt-Gr and Au-Gr layers results in a tighter binding at the Pt-Gr interface compared to the Au-Gr interface [15]. This binding also influences the electrical contact at the Pt-Gr interface, which remains intact even at high probe pull-off forces. Experimental confirmation of this behavior was observed at the probe break-off point from the graphene surface, where the probe-sample interaction force reached approximately $F \approx -625$ nN, under a relatively low applied voltage of $V_{\mathrm{app}} = \pm 0.4$ V, as shown in Figure 5a. As the probe is retracted from the sample, the electrical contact persists at the Pt-Gr interface. The high interaction forces in the Pt-Gr interface cause an increase in the distance between the Au and graphene layers, leading to the lifting of the graphene monolayer from the Au film.

With increase in the positive applied voltage, the charge redistribution in the system changes the electrical contact and the probe-sample interaction force. In the reverse bias state charge accumulation occurs in the Au-Gr interface, thus weakening the interaction between the Au and graphene layers. In turn, the interaction force in the Pt-Gr interface is relatively increased and is proved by the current I_{T} shift towards higher pull-off forces as the V_{app} is increased (Figure 5b).

3.4. Fermi Level Pinning in Charge Transport Model

Based on the findings from the earlier sections, it is evident that an asymmetry exists in the electrical current flow through the stacked metal-graphene-metal structure depending on the voltage polarity when gold and platinum metals are employed. The I-V characteristics of such a system exhibit diode-like behavior with forward and reverse bias states. Furthermore, when applied voltages exceed 1 V, the detach force, which is sensitive to charge distribution in the sample, is affected particularly when a positive voltage is applied to the gold electrode. Moreover, based on the probe retract experiments the interaction force between platinum SPM probe and graphene is stronger compared to the interaction between the graphene and the Au layer.

Taking into account these findings, the charge transport in gold-graphene-platinum structure can be explained as follows.

(1) In a low voltage regime ($< | \pm 0.7 |$ V) the charge flow is defined by the density of states in graphene near the Fermi level and electrical current value is independent of the polarity of the electrical field (Figure 6a).

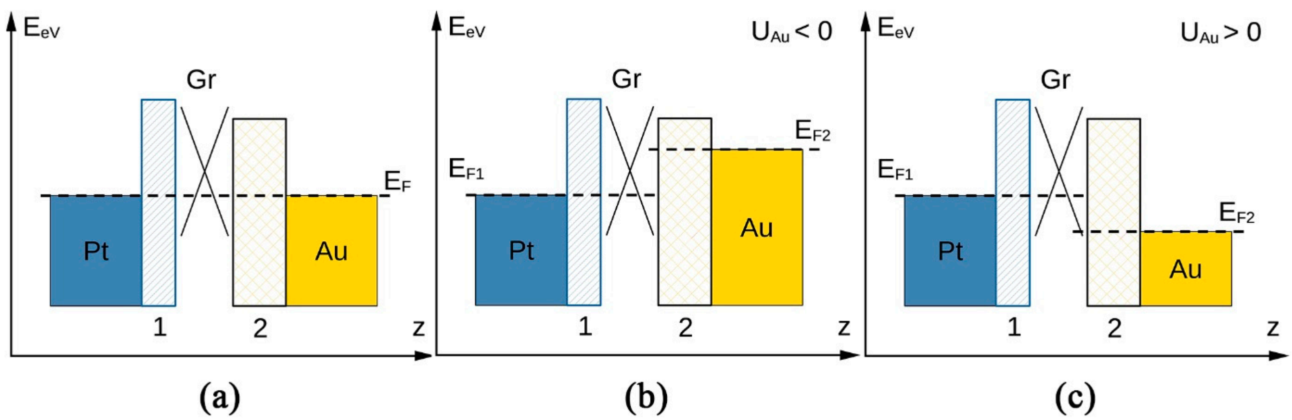

Figure 6. Scheme of a flat band model explaining the charge transfer mechanism in metal—graphene—metal system at the equilibrium (**a**) and under positive (**c**) and negative (**b**) voltages applied to the graphene supporting gold film. The top electrode is a flat Pt probe.

(2) In the forward bias regime, the transfer of electrons can be described as electrons flowing from the gold electrode into the graphene due to the occupation of free electronic states in graphene at energies higher than the Fermi level in the graphene-platinum stack. The interaction between graphene and platinum is characterized by a more intense electron sharing compared to the graphene-gold system. It can be suggested that the platinum-

graphene system can be analyzed as a component with the Fermi level fixed at the same position in both materials, as shown in Figure 6b. In other words, graphene's Fermi level may be pinned to the Pt electrode. Assuming the Fermi level pinning of graphene to the Pt probe, the electron density is determined by the balance between the redistribution of electrons between the free states in graphene and the platinum. As a result, the occupation of electronic states and the position of the Fermi level in graphene remains largely unaffected by the injection of additional electrons from the gold electrode.

(3) In the reverse bias regime, electron transport is hindered by the limited density of free states near the Fermi level in graphene. This limitation is attributed to the pinning effect observed in the platinum-graphene stacking configuration. As a result, the graphene layer acts as a blocking gate for voltages up to 0.5 V in the M-G-M system, impeding the flow of electrons in the reverse direction. The restricted electron transport arises from the limited availability of free electronic states in graphene. Fermi level pinning effect, due to the interaction between graphene and the Pt electrode, restricts the movement of electrons and hinders their transport in the reverse bias regime.

4. Conclusions

Electrical current and the interaction forces between the layers were investigated in the platinum–graphene–gold system produced via mechanical assemblage of the structure. The charge transport across the sandwich-like structure is determined via an asymmetrical distribution of the built-in charge across the metal–graphene–metal system.

In the system with different metallic electrodes, the current–voltage characteristics demonstrate different behavior for forward and reverse bias states. Under the forward bias, DC voltage applied across the sandwich structure space charge limits the increase in the electron transport. If the reverse bias voltage is applied, the current is practically constant up to some maximal voltages depending on the components of the structure. In the Pt–graphene–Au structure, diode-like current–voltage characteristics were measured in the interval between about -0.5 V and 0.5 V. The forward bias current was detected for the negative potential applied to the gold film with the graphene monolayer on top.

In the forward bias state, the charge transport was controlled via the injection of the electrons from the Au electrode into the graphene due to occupation of the free states of the graphene at energies significantly higher than the Fermi level in the graphene–Pt sandwich. A charge accumulation in the graphene was completely suppressed via fast extraction of the excess electrons from the graphene to the Pt. The extraction rate was obviously higher than the data acquisition time because no charging drift was detected. Instead of that, the interaction force between the probe and the graphene significantly increased especially if the voltages were $>|\pm 0.5|$ V. The reverse bias characteristics were detected for the positive Au and negative Pt probes in the M-G-M system. In the reverse bias state, the electron transport is restricted by the highly limited density of the free states in the vicinity of the Fermi level in the graphene due to the pinning effect in the Pt–graphene sandwich. The graphene layer functions as a blocking gate for the voltages from the tested interval in the M-G-M system. The charge transport can be changed by an increase in the compressing force of the Pt probe. The loading force is acceptable to change the charge transport for both the forward and the reverse bias current conditions.

Author Contributions: Conceptualization, T.D., V.B. and A.Š.; methodology, T.D., V.B. and A.Š.; formal analysis, A.Š.; investigation, T.D.; resources, V.B., A.L. and V.N.; writing—original draft preparation, T.D.; writing—review and editing, T.D., V.B. and A.Š.; visualization, A.Š., T.D. and V.B.; supervision, A.Š. All authors have read and agreed to the published version of the manuscript.

Funding: This research received no external funding.

Data Availability Statement: The data presented in this study are available upon request from the corresponding author.

Conflicts of Interest: The authors declare no conflict of interest.

References

1. Zhirnov, V.V.; Meade, R.; Cavin, R.K.; Sandhu, G. Scaling Limits of Resistive Memories. *Nanotechnology* **2011**, *22*, 254027. [CrossRef] [PubMed]
2. Yang, Q.; Zhang, Y.; Fu, Z.-Q.; Chen, Y.; Di, Z.; He, L. Creating Custom-Designed Patterns of Nanoscale Graphene Quantum Dots. *2D Mater.* **2022**, *9*, 021002. [CrossRef]
3. Zhao, X.; Zhang, X.; Chen, R.; Lang, H.; Peng, Y. Flexible Tuning of Friction on Atomically Thin Graphene. *ACS Appl. Mater. Interfaces* **2023**, *15*, 10315–10323. [CrossRef] [PubMed]
4. Liu, Y.; Weiss, N.O.; Duan, X.; Cheng, H.-C.; Huang, Y.; Duan, X. Van Der Waals Heterostructures and Devices. *Nat. Rev. Mater.* **2016**, *1*, 16042. [CrossRef]
5. Yang, M.; Liu, Y.; Fan, T.; Zhang, D. Metal-Graphene Interfaces in Epitaxial and Bulk Systems: A Review. *Prog. Mater. Sci.* **2020**, *110*, 100652. [CrossRef]
6. Gong, C.; Lee, G.; Shan, B.; Vogel, E.M.; Wallace, R.M.; Cho, K. First-Principles Study of Metal–Graphene Interfaces. *J. Appl. Phys.* **2010**, *108*, 123711. [CrossRef]
7. Khomyakov, P.A.; Giovannetti, G.; Rusu, P.C.; Brocks, G.; van den Brink, J.; Kelly, P.J. First-Principles Study of the Interaction and Charge Transfer between Graphene and Metals. *Phys. Rev. B* **2009**, *79*, 195425. [CrossRef]
8. Chaves, F.A.; Jiménez, D.; Cummings, A.W.; Roche, S. Physical Model of the Contact Resistivity of Metal-Graphene Junctions. *J. Appl. Phys.* **2014**, *115*, 164513. [CrossRef]
9. Passi, V.; Gahoi, A.; Marin, E.G.; Cusati, T.; Fortunelli, A.; Iannaccone, G.; Fiori, G.; Lemme, M.C. Ultralow Specific Contact Resistivity in Metal–Graphene Junctions via Contact Engineering. *Adv. Mater. Interfaces* **2019**, *6*, 1801285. [CrossRef]
10. Song, A.; Shi, R.; Lu, H.; Gao, L.; Li, Q.; Guo, H.; Liu, Y.; Zhang, J.; Ma, Y.; Tang, X.; et al. Modeling Atomic-Scale Electrical Contact Quality Across Two-Dimensional Interfaces. *Nano Lett.* **2019**, *19*, 3654–3662. [CrossRef] [PubMed]
11. Yoon, H.H.; Ahmed, F.; Dai, Y.; Fernandez, H.A.; Cui, X.; Bai, X.; Li, D.; Du, M.; Lipsanen, H.; Sun, Z. Tunable Quantum Tunneling through a Graphene/Bi_2Se_3 Heterointerface for the Hybrid Photodetection Mechanism. *ACS Appl. Mater. Interfaces* **2021**, *13*, 58927–58935. [CrossRef] [PubMed]
12. Papadopoulos, N.; Gehring, P.; Watanabe, K.; Taniguchi, T.; van der Zant, H.S.J.; Steele, G.A. Tunneling Spectroscopy of Localized States of WS2 Barriers in Vertical van Der Waals Heterostructures. *Phys. Rev. B* **2020**, *101*, 165303. [CrossRef]
13. Iordanidou, K.; Mitra, R.; Shetty, N.; Lara-Avila, S.; Dash, S.; Kubatkin, S.; Wiktor, J. Electric Field and Strain Tuning of 2D Semiconductor van Der Waals Heterostructures for Tunnel Field-Effect Transistors. *ACS Appl. Mater. Interfaces* **2023**, *15*, 1762–1771. [CrossRef] [PubMed]
14. Gong, C.; Hinojos, D.; Wang, W.; Nijem, N.; Shan, B.; Wallace, R.M.; Cho, K.; Chabal, Y.J. Metal–Graphene–Metal Sandwich Contacts for Enhanced Interface Bonding and Work Function Control. *ACS Nano* **2012**, *6*, 5381–5387. [CrossRef]
15. Vanin, M.; Mortensen, J.J.; Kelkkanen, A.K.; Garcia-Lastra, J.M.; Thygesen, K.S.; Jacobsen, K.W. Graphene on Metals: A van Der Waals Density Functional Study. *Phys. Rev. B* **2010**, *81*, 081408. [CrossRef]
16. Nam Do, V.; Anh Le, H. Transport Characteristics of Graphene-Metal Interfaces. *Appl. Phys. Lett.* **2012**, *101*, 161605. [CrossRef]
17. Sakavičius, A.; Agafonov, V.; Bukauskas, V.; Daugalas, T.; Kamarauskas, M.; Lukša, A.; Nargelienė, V.; Niaura, G.; Treideris, M.; Šetkus, A. Long-Time Drift Induced Changes in Electrical Characteristics of Graphene–Metal Contacts. *Lith. J. Phys.* **2020**, *60*, 235–246. [CrossRef]
18. Babcock, K.L.; Prater, C.B. *Phase Imaging: Beyond Topography*; Digit Instruments: St. Barbar, CA, USA, 1995.
19. Daugalas, T.; Bukauskas, V.; Lukša, A.; Nargelienė, V.; Šetkus, A. Intentionally Created Localized Bridges for Electron Transport through Graphene Monolayer between Two Metals. *Nanotechnology* **2022**, *33*, 375402. [CrossRef]
20. Daugalas, T.; Bukauskas, V.; Lukša, A.; Nargelienė, V.; Šetkus, A. Relationship between Changes in Interface Characteristics and External Voltage under Compressing Force in Metal–Graphene–Metal Stacks. *J. Phys. D Appl. Phys.* **2023**, *56*, 345305. [CrossRef]
21. Zhang, P.; Li, J.-T.; Meng, J.-W.; Jiang, A.-Q.; Zhuang, J.; Ning, X.-J. Conductivity of Graphene Affected by Metal Adatoms. *AIP Adv.* **2017**, *7*, 035101. [CrossRef]